

# Improving Results of CVFEM with the FLO scheme applied to Heat and Fluid Flow Problems

Mostefa KAOUARI<sup>\*1</sup>, Fodil HAMMADI<sup>\*2</sup>, Belkacem DRAOUI<sup>#3</sup>, Aïcha CHOUBANE<sup>\*2</sup>

<sup>\*</sup>Laboratory of Mechanics: Simulation & experimentation (L2ME), TAHRI Mohamed University of Bechar, ALGERIA.

<sup>#</sup> ENERGARID Laboratory, TAHRI Mohamed University of Bechar, ALGERIA.

<sup>1</sup>Kaouari\_must@yahoo.fr

<sup>2</sup>h\_fodil@yahoo.fr

<sup>3</sup>bdraoui@yahoo.fr

<sup>4</sup>icha213@yahoo.fr

**Abstract** — Now CVFEM is more attractive as method for solving real problems in CFD. Combining advantages of CVFDMs and those of FEMs produce a new one, able to deal with complexes geometries, and satisfy local and global conservation principals. To solve dynamical field, good scheme is always required for discretization of the convection terms. The FLO scheme is adopted in this study because it is extracted as exact solution from a modified equation. The procedure of resolution used is the SIVA. Programming this procedure with advanced instructions Fortran 90/95. The results presented, prove a best agreement with benchmarks.

**Keywords** — CVFEM, convection terms, FLO scheme, SIVA, Fortran 90/95.

## I. INTRODUCTION

Control Volume Finite Element Method (CVFEM) is more popular for solving problems of fluid flow and heat transfer with different degrees of complexities. The success reached in mixing the two ancient methods (CVFDM and FEM) in CFD problems increase the field of its applicability. The physical domain is discretized in three nodes triangular elements; every element is subsequently divided in three subvolumes, this geometrical treatment is achieved by collecting all subvolumes surrounding the considered node to construct the control volume. Much other geometrical information is needed for the discretization of conservation and continuity equations step.

Convective terms present in the momentum equations are very difficult to handle it without specific considerations. These convection terms are approximated by interpolation function that responds to an element Peclet number and take account the direction of the element average velocity vector. The diffusion terms are interpolated linearly, and there is no reason to use the same scheme used for convection ones. The first eminent work that presents the FLO scheme is Baliga and Patankar [4-5], the ideas behind this scheme was proposed in the work of Raithby [10-12].

All works in the literature propose computing velocities components and pressure in different places in the grid, using staggered grid in structured grid, Patankar and Spalding [2], Harlow and Welch [3], and many other works, or using unequal order or computing pressure at element centroid in the case of unstructured grid. This difficulty was solved by the work of Rhie and Chow [12], and its adaptation for unstructured grid was proposed by Prakash and Patankar [6]. Equal-order method allows using one single mesh and the discretization satisfies the masse conservation.

## II. GOVERNING EQUATIONS

This work is limited to steady flows of incompressible Newtonian fluids. The governing equations of continuity or momentum are given by non-linear partial differential equations expressed in Cartesian coordinates system (x, y):

A. Continuity Equation:

$$\frac{\partial(\rho u_i)}{\partial x_i} = 0 \quad (1)$$

B. Momentum Equations:

$$\frac{\partial(\rho u_i)}{\partial t} + \frac{\partial(\rho u_i u_j)}{\partial x_j} = -\frac{\partial P}{\partial x_i} + \frac{\partial}{\partial x_j} \left( \mu \frac{\partial u_i}{\partial x_j} \right) + S_{u_i} \quad (2)$$

C. Transport Equation for other scalar variable:

$$\frac{\partial(\rho \phi)}{\partial t} + \frac{\partial(\rho u_i \phi)}{\partial x_i} = \frac{\partial}{\partial x_i} \left( \Gamma_\phi \frac{\partial \phi}{\partial x_i} \right) + S_\phi \quad (3)$$

## III. NUMERICAL METHOD

The CVFEM used in the procedure of discretization of the aforementioned equations, allows converting these equations in system of algebraic equations by integration on control volume surrounding the considered node of the calculation domain.

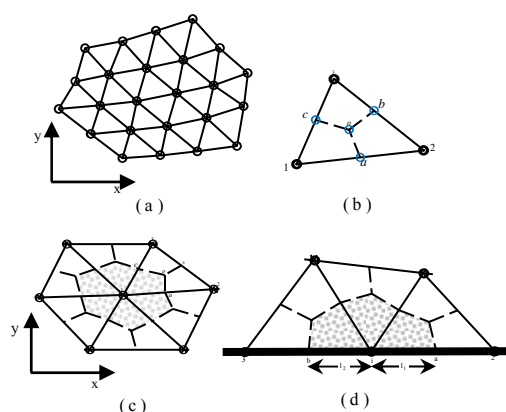


Fig. 1 Discretization of calculation domain and nomenclatures: (a) simple domain decomposed on triangular elements; (b) triangular element and its calculated necessary positions; (c) a cell designated by an internal node  $i$  and all its surrounding elements, control volume associate with it; (d) elements and control volume associated at node  $i$  on the boundary.

A. Transport Equation of  $\phi$  (general form):

Considering a node from a calculating domain, and applied all the principals of integrating inherent to the

method on terms of momentum and continuity equations, all contributions are collected with respect to the element-by-element basis, without forgetting terms related to boundary contributions if they exist.

$$\int_{\text{iaoc}} \frac{\partial}{\partial t} (\rho\phi) dV + \int_a \bar{J} \cdot \bar{n} ds + \int_o \bar{J} \cdot \bar{n} ds - \int_{\text{iaoc}} S_\phi dV \quad (4)$$

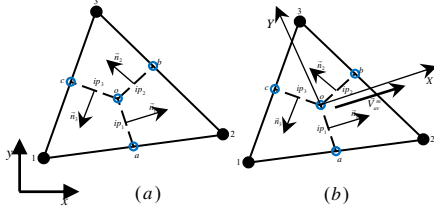


Fig. 2 (a) designation of integration point's \$ip\_i\$ on the faces \$an\$ and the associated unity vectors \$\bar{n}\_i\$ on the global coordinate system; (b) visualization of local axes system on the element centroïde, \$X\$ axe is parallel to \$\bar{v}\_{av}^m\$

The flux \$\bar{J}\$ is a combination of two existent fluxes in the principal equation, the diffusion flux \$\bar{J}\_D\$ and the convection flux \$\bar{J}\_C\$. \$\bar{n}\$ is normal vector to the face (one among three), \$ds\$ designate its length, fig.2(a).

$$\bar{J} = \bar{J}_D + \bar{J}_C \quad (5)$$

$$\bar{J}_D = -\Gamma_\phi \nabla \phi \quad (6)$$

$$\bar{J}_C = \rho \bar{v} \phi \quad (7)$$

The source term \$S\_\phi\$ is always expressed under the linear form, \$S\_p\$ and \$S\_c\$ are computed at nodes of the calculated domain and there values are assumed to prevail on the portion of the volume belong to the considering node.

$$S_\phi = S_p \phi + S_c \quad (8)$$

## B. Interpolation functions:

### B.1. Diffusion term:

On each element, the dependent variable \$\phi\$ in diffusion term is interpolated linearly:

$$\phi = A_\phi^D x + B_\phi^D y + C_\phi^D \quad (9)$$

The values of coefficients \$A\_\phi^D\$, \$B\_\phi^D\$ and \$C\_\phi^D\$, can be uniquely expressed in terms of three nodal values of \$x\$, \$y\$ and \$\phi\$ for each element.

### B.2. Convection term:

For convection terms, the scheme of Saabas and Baliga [7-9, 5], and others is used in this work. Because of strong convection relative to moderate diffusion transport can happened, linear interpolation of the advection term lead to unrealistic oscillatory solution or divergence of all the iterative solution procedure.

$$\phi^C = A_\phi^C \xi + B_\phi^C Y + C_\phi^C \quad (10)$$

$$\xi = \frac{\Gamma_\phi}{\rho U_{av}^m} \left[ \exp\left(\frac{P_e (X - X_{max})}{X_{max} - X_{min}}\right) - 1 \right] \quad (11)$$

$$P_e = \frac{\rho U_{av}^m (X_{max} - X_{min})}{\Gamma_\phi} \quad (12)$$

$$\begin{cases} X_{max} = \text{MAX}(X_1, X_2, X_3) \\ X_{min} = \text{MIN}(X_1, X_2, X_3) \end{cases} \quad (13)$$

The new local axes system \$(X, Y)\$ is oriented parallel to the direction of \$\bar{v}\_{av}^m\$ fig. 2(b). The variable \$\xi\$ present in equation (11) express exponential variations in the flow direction. Coefficients \$A\_\phi^C\$, \$B\_\phi^C\$ and \$C\_\phi^C\$ are functions of nodal values of \$\phi\$, \$Y\$ and \$\xi\$.

$$U_{av}^m = |\bar{v}_{av}^m| \quad (14)$$

$$\bar{v}_{av}^m = u_{av}^m \bar{i} + v_{av}^m \bar{j} \quad (15)$$

$$u_{av}^m = \frac{u_1^m + u_2^m + u_3^m}{3}; \quad v_{av}^m = \frac{v_1^m + v_2^m + v_3^m}{3} \quad (16)$$

### B.3. Discretization of \$\phi\$ equation:

Now all the necessary ingredients are present to apply integration on the three faces insight the element. However, it is important to mention that diffusion terms are integrated directly, but advection terms are integrated by mean of Simpson1/3. The final algebraic expression for node \$i\$ is obtained assembling procedure for all elements contributions sharing the same node:

$$a_i^\phi \phi_i = \sum_{nb} a_{nb}^\phi \phi_{nb} + b_i^\phi \quad (17)$$

$$a_i^\phi = \sum_{nb,i} a_{nb,i}^\phi - \sum_{\text{elem.assoc. with } i} \left( S_{p,i}^\phi \right)_{\text{elem}} \quad (18)$$

$$b_i^\phi = \sum_{\text{elem.assoc. with } i} \left( S_{c,i}^\phi \cdot V_{\text{elem}} / 3 \right) \quad (19)$$

### B.4. Discretization of momentum equations:

Thus it is seen that a clear similarity between momentum equations and general form equation of transported scalar \$\phi\$, except existence of additional terms of pressure gradients in momentum equations. For less programming effort, it is advantageous and rational to implement only one general procedure, and careful for adding adequate terms if necessary like eq. (20). Finally, apply the assembly procedure for obtaining algebraic equations given in there compact form eq. (21):

$$\int_{\text{iaoc}} \left( -\frac{\partial p}{\partial x_j} \right) dV = - \left( \frac{\partial p}{\partial x_j} \right)_{\text{elem}} V_{\text{iaoc}} \quad (20)$$

$$a_i^{u_j} (u_j)_i = \sum_{nb} a_{nb}^{u_j} (u_j)_{nb} + b_i^{u_j} - \left( \frac{\partial p}{\partial x_j} \right) \cdot V_i \quad (21)$$

Additional terms \$\overline{(\partial p / \partial x\_j)} \cdot V\_i\$ represent volume averaged pressure-gradients associated with the control volume surrounding node \$i\$.

$$(u_j)_i = (\hat{u}_j)_i - d_i^{u_j} \left( \frac{\partial p}{\partial x_j} \right) \quad (22)$$

$$(\hat{u}_j)_i = \frac{\sum_{nb} a_{nb}^{u_j} (u_j)_{nb} + b_i^{u_j}}{a_i^{u_j}} \quad (23)$$

$$d_i^{u_j} = \frac{V_i}{a_i^{u_j}} \quad (24)$$

The interpolation functions used to approximates components of velocities in the mass-flux terms are defined as:

$$\mathbf{u}_i^{mj} = \hat{\mathbf{u}}_i^j - \mathbf{d}_o^{uj} \left( \frac{\partial \mathbf{p}}{\partial X_i^j} \right)_{\text{elem}} \quad (25)$$

#### B.5. Equation de pression :

The contribution of an element to the mass conservation equation for a control-volume surrounding node  $i$  can be written as:

$$\int_a^o \rho \bar{\mathbf{V}}^m \cdot \bar{\mathbf{n}} ds + \int_o^c \rho \bar{\mathbf{V}}^m \cdot \bar{\mathbf{n}} ds \quad (26)$$

However, it is important to note that pressure must be expressed by its interpolation function which have a linear form, pressure gradients are exactly the coefficients of the pressure interpolation function.

$$p = A^P x + B^P y + C^P \quad (27)$$

In the same manner to the  $\phi$  coefficients, here too, the coefficients of the interpolation function are themselves functions of nodal pressure of the considered element and coordinates of these same element nodes.

After integration on faces insight the element and a suitable assembling procedure of all contributions of all other elements surrounding node  $i$ , the algebraic equations are obtained and written in its compact form as:

$$\mathbf{a}_i^P \mathbf{p}_i = \sum_{nb} \mathbf{a}_{nb}^P \mathbf{p}_{nb} + \mathbf{b}_i^P \quad (28)$$

$$\text{where, } \mathbf{a}_i^P = \sum_{nb} \mathbf{a}_{nb}^P \quad (29)$$

#### B.6. Boundary conditions:

To close all contributions for obtaining the final algebraic equations, boundary conditions must be included properly.

If the value of dependent variable is specified on a portion of the boundary, than the suitable treatment is as:

$$\mathbf{a}_i^\phi = 1, \mathbf{a}_{nb}^\phi = 0, \mathbf{b}_i^\phi = \phi_{\text{spec}} \quad (30)$$

If the known transported scalar is a component of velocity, additional treatment is made, the coefficient of pressure gradient become null and pseudo-velocity obtain the velocity value.

For specified flux condition, the total flux of  $\phi$  normal to the boundary is given by the expression:

$$\bar{\mathbf{J}} \cdot \bar{\mathbf{n}} = \rho \mathbf{V}_n \phi - \Gamma_\phi \left( \frac{\partial \phi}{\partial n} \right)_{\text{spec}} \quad (31)$$

If outflow condition is considered, the diffusion term is negligible compared to the convection term, for this reason the term  $\Gamma_\phi \left( \frac{\partial \phi}{\partial n} \right)$  is eliminated from equation.

#### B.7. Under-relaxation:

Following proposition of Patankar [1], under-relaxation is a very useful tool to handle the strong non-linearity found in discretized equations of Navier-Stokes equations, the values of dependent variables change hugely from iteration to the successive one. The E-factor method is retained in the code developed in the context of this work. The values of E proposed are 1 for the components of velocity and pressure, and 5 for temperature.

$$\mathbf{a}_i^{uj} \left( 1 + \frac{1}{E^i} \right) (\mathbf{u}_j)_i = \sum_{nb} \mathbf{a}_{nb}^{uj} (\mathbf{u}_j)_{nb} + \mathbf{a}_j^P \mathbf{P}_j + \sum_{nb} \mathbf{a}_{nb}^P \mathbf{P}_{nb} + \mathbf{b}_i^{uj} + \frac{\mathbf{a}_{i,j}^{uj}}{E^i} (\mathbf{u}_j)_i \quad (32)$$

## IV. ALGORITHME DE RESOLUTION

The acronym SIVA ‘‘Sequential Iterative Variable Adjustment’’ is the procedure of solution adopted in this work because its implementation is very simple. It is not necessary to repeat all the steps of the algorithm here. The reader is invited urgently to the documents founded in literature, to see details needed.

## V. TESTS DE VALIDATION

### A. Lid driven cavity :

This benchmark is an important two-dimensional laminar incompressible fluid flow. The fluid is moved by a horizontal velocity on the upper wall, while the other three are subject to the adhesion condition. This problem depends on the values of Reynolds number which can give dominance to the convection terms when its value is higher enough. Moreover, there are two singularities located on the bottom corners of the cavity, locations where arise secondary recirculation cells in addition to the primary cell that dominate the majority of the space of the cavity. The geometry of the problem is as shown in fig. 3.

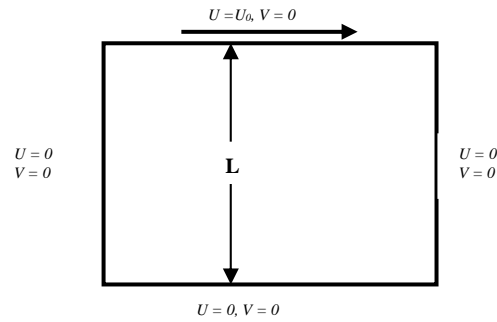


Fig. 3: Driven cavity geometry, and boundary conditions.

The results obtained are compared to those of Ghia et al. [18] and L. D. Tran et al. [14]. A comparative table is drawn below tab. 1 to show the superiority of results of this work against those given by works of L. D. Tran et al. [14].

Tab. 1 COMPARISON OF RESULTS,  $Re = 400$ .

Scheme	Grid	$U_{\min}$	$V_{\max}$	$V_{\min}$
Tran et al.	32x32	-.25841	.24042	-.37622
Present work		-.28096	.25876	-.39411
Tran et al.	64x64	-.30192	.27823	-.42476
Present work		-.30903	.28525	-.43168
Tran et al.	129x129	-.32052	.29548	-.44475
Present work		-.32286	.29824	-.44743
<b>Ghia et al.</b>	129x129	-.3273	.3020	-.4499

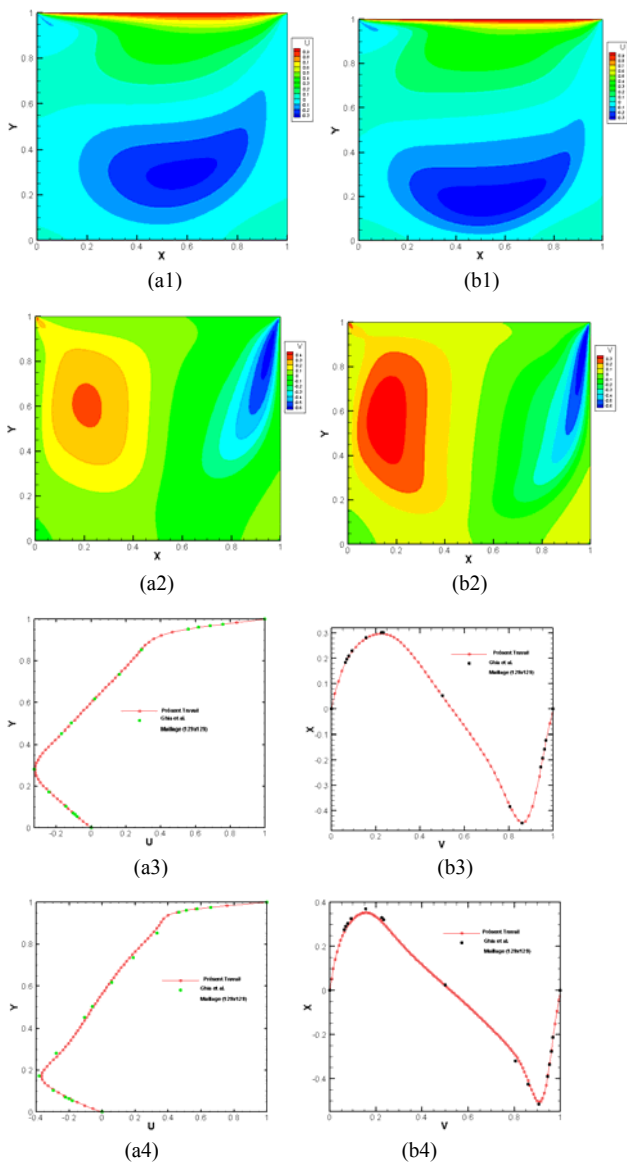


Fig. 4: Display velocity components fields  $u$  and  $v$ ,  $Re=400$  (a1), (a2);  $Re = 10^3$  (b1) and (b2). Display of velocity profiles for  $u$  at  $x=0.5$  and  $v$  at  $y=0.5$  (a3), (b3) for  $Re = 400$ , and (a4) and (b4) for  $Re = 10^3$ .

**B. Natural Convection:**

A square cavity side  $L$  containing fluid in motion caused by a difference in temperature between the two sides right and left one. The two other sides are adiabatic, see fig. 5. This difference temperature excites the fluid to circulate into the cavity. The Boussinesq hypothesis is valuable here. The Prandtl number has the value 0.72 and the Rayleigh number varies between  $10^3$  and  $10^6$ . Here too, the code built in this work prove its superiority, its results are very close to those of De Vahl Davis [15] than those given by the works of Wan et al. [17] and Véronique Feldheim [16], tab.2 and tab.3 confirm these findings:

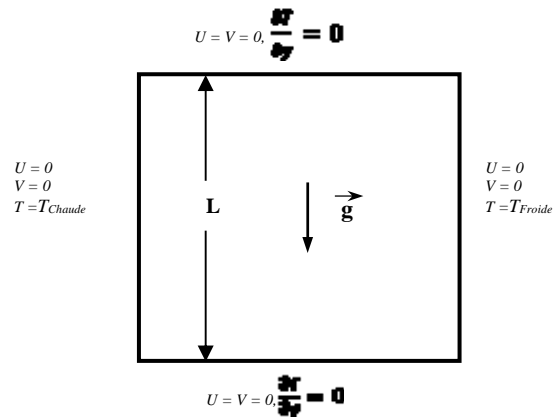


Fig. 5: Natural convection cavity and boundary conditions.

TAB.2 COMPARISON OF RESULTS,  $Ra = 10^3$  AND  $10^4$ .

$Ra = 10^3$	$U_{max}$	$V_{max}$	$Ra = 10^4$	$U_{max}$	$V_{max}$
<b>De Vahl Davis, 1983</b>	<b>3.649</b>	<b>3.697</b>		<b>16.178</b>	<b>19.617</b>
Wan et al.,2001 (DSC)	3.643	3.686		15.967	19.98
Wan et al.,2001 (FEM)	3.489	3.686		16.122	19.79
<b>Véronique Feldheim</b>					
41x41	3.629	3.674	41x41	16.025	19.610
81x81	3.644	3.689	81x81	16.077	19.703
161x161	3.649	3.692	161x161	16.098	19.730
<b>Present Work</b>					
33x33	3.6418	3.6842	33x33	16.056	19.5724
81x81	3.6483	3.6954	81x81	16.1643	19.5999
161x161	3.6492	3.6964	161x161	16.1746	19.6348

TAB.3: COMPARISON OF RESULTS,  $Ra = 10^5$  AND  $10^6$ .

$Ra = 10^5$	$U_{max}$	$V_{max}$	$Ra = 10^6$	$U_{max}$	$V_{max}$
<b>De Vahl Davis, 1983</b>	<b>34.73</b>	<b>68.59</b>		<b>64.63</b>	<b>219.36</b>
Wan et al., 2001 (DSC)	33.51	70.81		65.55	227.24
Wan et al., 2001 (FEM)	33.39	70.63		65.40	227.11
<b>Véronique Feldheim</b>					
41x41	33.73	70.09	41x41	65.19	225.06
81x81	33.52	70.251	81x81	65.397	226.60
161x161	33.443	70.549	161x161	65.418	226.62
<b>Present Work</b>					
33x33	33.936	68.679	33x33	60.1161	215.666
81x81	34.544	68.613	81x81	63.7264	220.660
161x161	34.633	68.654	161x161	64.4546	220.786

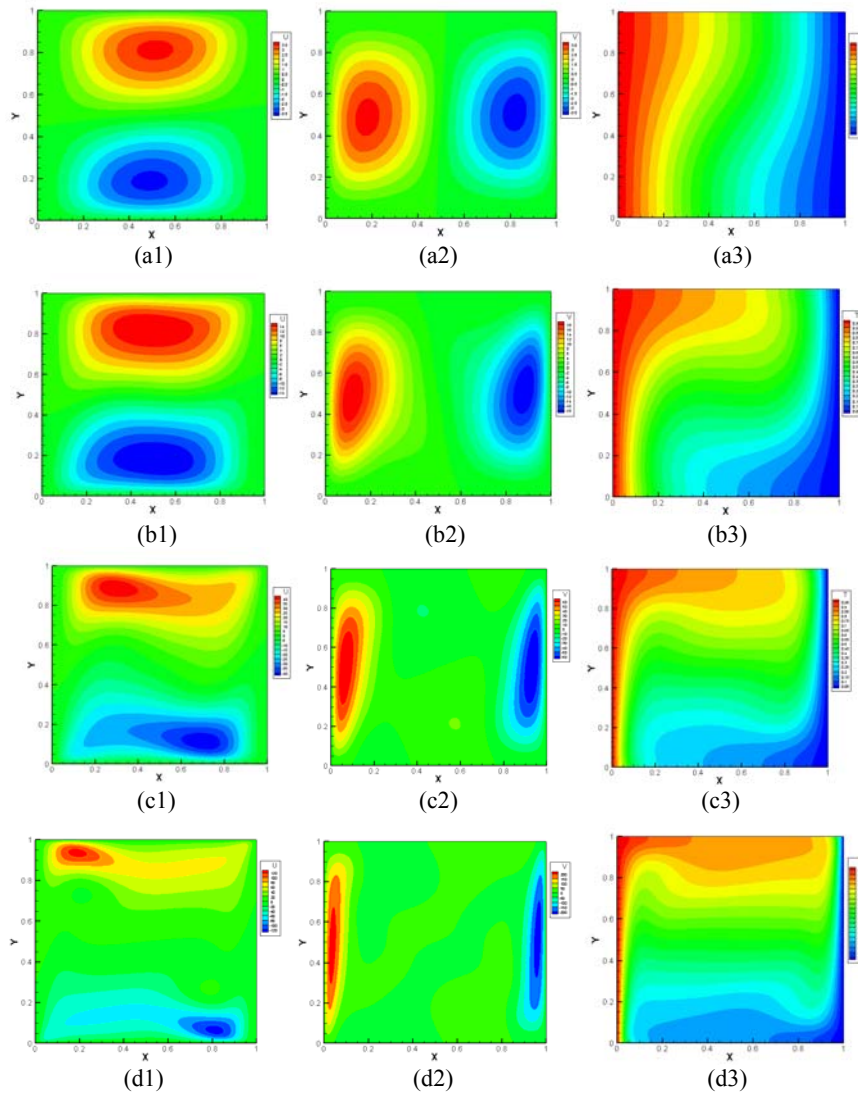


Fig. 6: Fields of velocity components  $u$ ,  $v$  and temperature  $T$  for different values of Rayleigh.  $Ra = 10^3$  on figure (a1), (a2) and (a3).  $Ra = 10^4$  on figure (b1), (b2) and (b3).  $Ra = 10^5$  on figure (c1), (c2) and (c3).  $Ra = 10^6$  on figure (d1), (d2) and (d3).

## VI. CONCLUSIONS

During the elaboration of this work, the aim was reproduction of Saabas work [7-9, 5] mentioned in many references; the idea is to see the impact of advanced object-oriented programming with Fortran 90/95 language on the quality of results.

Despite recent criticisms made in the work of A. Lamoueux et al. [13], the obtained results show superiority compared to those found in the literature. Moreover, the implementation of algorithm of solution is simple and direct, and no need for necessary correction of velocity components or pressure. The only existent inconvenient in the procedure of solution is the affectation of zero value to the coefficients of pressure gradients at the boundary where the velocity components are known.

## REFERENCES

- [1] Patankar, S. V., Numerical Heat Transfer and Fluid Flow, Hemisphere / McGraw Hill New York, 1980.
- [2] Patankar, S. V. and Spalding, D. B., A Calculation Procedure for Heat, Mass and Momentum Transfer in Three-Dimensional Parabolic Flows, Int. J. Heat Mass Transfer, Vol. 15, pp. 1787-1806, 1972.
- [3] Harlow, F. H. and Welch, J. E., Numerical Calculation of Time-Dependent Viscous Incompressible Flow of Fluid with a Free Surface, Phys. Of Fluids, Vol. 8, pp. 2182-2189, 1965.
- [4] Baliga, B. R., A Control-Volume Based Finite Element Method for Convective Heat and Mass Transfer, Ph.D. Thesis, University of Minnesota, Minneapolis, U.S.A., 1978.
- [5] B. R. Baliga and S. V. Patankar, A New Finite-Element Formulation for Convection- Diffusion Problems, Numer. Heat Transfer, vol. 3, no. 4, pp. 393-409, 1980.
- [6] Prakash C. and Patankar, S. V., A Control-Volume-Based Finite-Element Method for Solving the Navier-Stokes Equations Using Equal-Order Velocity-Pressure Interpolation, Numer. Heat Transfer, Vol. 8, pp. 259-280, 1985.
- [7] Saabas, H. J., A Control-Volume Finite Element Method for Three-Dimensional, Incompressible, Viscous Fluid Flow, Ph.D. Thesis, McGill University, Montreal, Canada, 1991.
- [8] Saabas, H. J. and Baliga, B. R., A Co-Located Equal-Order Control-Volume Finite Element Method for Multidimensional, Incompressible Fluid Flow - Part I: Formulation, Numer. Heat Transfer, Part A, Vol. 26, pp. 381-407, 1994.
- [9] Saabas, H. J. and Baliga, B. R., A Co-Located Equal-Order Control-Volume Finite Element Method for Multidimensional,

- Incompressible Fluid Flow - Part II: Verification, Numer. Heat Transfer, Part B, Vol. 26, pp. 409-424, 1994.
- [10] G. D. Raithby, A Critical Evaluation of Upstream Differencing Applied to Problems Involving Fluid Flow, Comput. Methods Appl. Mech. Eng., vol. 9, no. 1, pp. 75-103, 1976.
- [11] G. D. Raithby, Skew Upstream Differencing Schemes for Problems Involving Fluid Flow, Comput. Methods Appl. Mech. Eng., vol. 9, 2, pp. 153-164, 1976.
- [12] Rhie, C. M. and Chow, W. L., Numerical Study of the Turbulent Flow Past an Airfoil with Trailing Edge Separation, MAA Journal, Vol. 21, pp. 1525-1532, 1983.
- [13] A. Lamoureux, B. R. Baliga, Improved Formulations of the Discretized Pressure Equation and Boundary Treatments in Co-located Equal-Order Control-Volume Finite Element Methods for Incompressible Fluid Flow, Numer. Heat Transfer, B, Vol. 59, pp. 442-472, 2011.
- [14] Luu Dung Tran, Christian Masson, and Arezki Smaïli, A Stable Second-Order Mass-Weighted Upwind Scheme for Unstructured Meshes, Int. Journal For Numer. Meth Fluids, Vol. 51: pp. 749-771, 2006.
- [15] Vahl Davis, G., Natural Convection of Air in a Square Cavity: A Benchmark Numerical Solution, Int. J. Num. Meth. Fluids, Vol. 3, pp. 249-264, 1983.
- [16] Véronique Feldheim, Simulation Numérique des Transferts Thermiques Combinés Conduction, Convection, Rayonnement dans des Domaines de Géométrie Complexe, Docteur en Sciences Appliquées, Faculté Polytechnique de Mons, 2002
- [17] Wan, D., Patnaik, B., and Wei, G., A New Benchmark Quality Solution for the Buoyancy-Driven cavity by Discrete Singular Convolution. Numer. Heat Transfer, Part B(40), pp. 199-228, 2001.
- [18] U. Ghia, K. N and C. Ghia, T. Shin, High-Re Solutions for Incompressible Flow Using the Navier-Stokes Equations and a Multigrid Method; J. Compu. Phys. Vol. 48; pp: 387-411, 1982.